MICRO COMBINED COOLING AND POWER

Kyle Gluesenkamp, Oak Ridge National Laboratory, Oak Ridge, TN
Reinhard Radermacher, Yunho Hwang, Center for Environmental Energy Engineering, University of Maryland, College Park, MD, USA, gluesenkampk@ornl.gov

Abstract: Thermally driven chillers can be driven by waste heat from prime movers (engines, turbines or fuel cells) to form combined cooling and power (CCP) systems. In this chapter, a method of matching chillers to prime movers is presented. CCP configurations with and without backup cooling are described, along with first-order estimates of the energy efficiency of each combination of configuration and prime mover. Some experimental results for micro combined cooling heating and power (CCHP) are presented. Based on the analytical and experimental work, it is concluded that CCP and CCHP performance depend heavily on the choice of prime mover. CCP systems based on fuel cells can use less energy than grid-driven electrical cooling systems. CCP with combustion-based prime movers has potential to save energy in off grid applications.

Key Words: prime mover, trigeneration, CCP, CCHP, CHP

1 INTRODUCTION

An important use for thermally driven chillers is to combine them with electricity production for co-production of cooling and power. When do such combined cooling and power (CCP) systems save primary energy compared to conventional, separate systems? This question can be addressed as a function of several important variables. In a first-order analysis, the efficiencies of a particular prime mover and a particular chiller can be treated as constant. This type of analysis is sufficient to reveal broad trends about combined cooling and power systems based on different prime movers. It provides perspective on technology potential and limitations, and a fundamental metric against which experimental results can be compared.

This chapter emphasizes micro-scale prime movers (<5 kW_{elec}), although some are included that are not available at this size range (microturbines and molten carbonate fuel cells). The analysis is applicable to any size system by referring to the underlying expressions (Gluesenkamp 2012) and substituting the component efficiencies desired by the reader. Internal and external combustion-based prime movers become significantly more efficient at larger scale, while the efficiency of fuel cells will be relatively constant.

This chapter also emphasizes combined cooling and power (CCP). Similar important possibilities exist, with the same basic equipment, for combined thermally driven heat pumping and power, or for combined cooling, heating and power (CCHP). For simplicity, the focus of this chapter remains on CCP, with some recent results for residential CCHP presented at the end of the chapter.

2 MATCHING PRIME MOVERS AND THERMALLY DRIVEN CHILLERS

One essential element for combined cooling and power is matching prime mover waste heat resources with thermally driven chiller requirements. A convenient tool for this analysis is the temperature vs. cumulative heat transfer (T-Q) diagram. The composite curve, a concept from pinch analysis which combines all forms of heat into a single line or curve (Kemp 2007), is shown for the waste heat resources of several micro-scale prime movers in Figure 1

(Gluesenkamp 2012). The prime movers shown are the spark ignition internal combustion engine (SI-ICE), molten carbonate fuel cell (MCFC), compression ignition internal combustion engine (CI-ICE), solid oxide fuel cell (SOFC), microturbine (MT), Stirling engine (SE), organic Rankine cycle (ORC), high temperature proton exchange membrane fuel cell (HT-PEMFC), and low temperature proton exchange membrane fuel cell (LT-PEMFC).

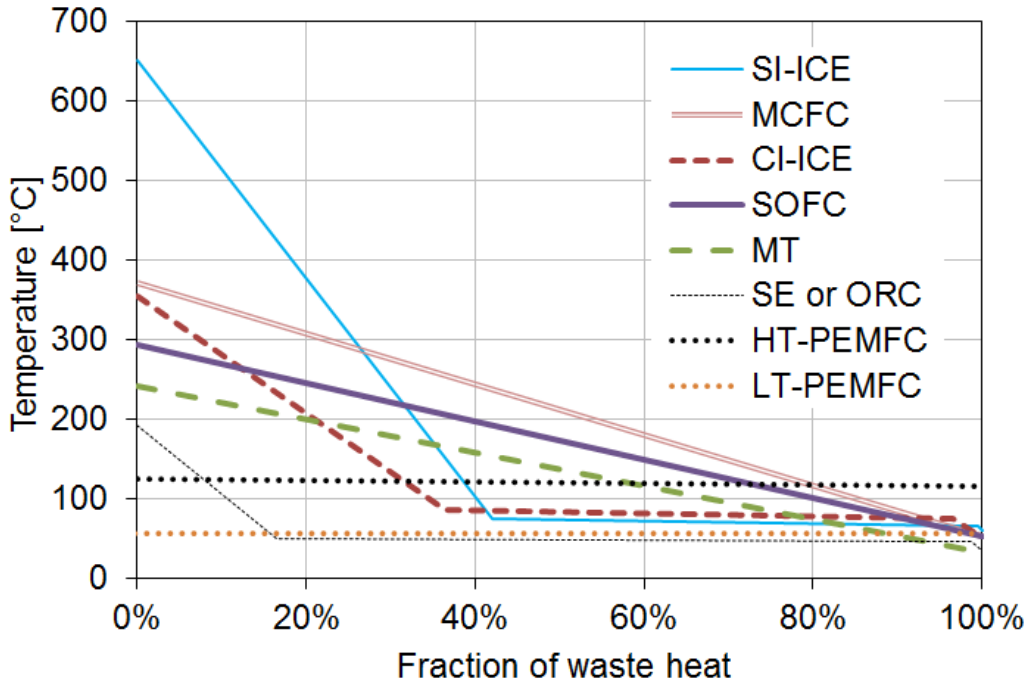

Figure 1: Waste heat resources for several micro prime movers

Figure 1 shows how much of each prime mover's waste heat is available at a given temperature. For example, about 67% of waste heat for a MT, 40% for a SI-ICE, and 0% for a LT-PEMFC are available above 100°C. The MT can provide about 83% of its waste heat above 60°C, compared to 100% for the SI-ICE and 100% for the LT-PEMFC.

The different thermally driven cooling options are shown in Figure 2 (Gluesenkamp and Radermacher 2011). Each technology covers a range of temperatures, since the driving temperature will change with external conditions. Most technologies are characterized by a narrow range of thermal COP. The region in the figure for adsorption cycles covers a very wide range of both temperature and COP since that region represents a wide diversity of working pairs. In general, when higher driving temperature is available, a higher COP technology can be used.

One way to show the match between prime movers and chillers is shown in Figure 3. Figure 3 places each prime mover on a plot of its electrical efficiency vs. the product $\varepsilon_{exh}COP_{th}$. COP_{th} is the thermal COP of the matching chiller, and ε_{exh} is the exhaust heat recovery effectiveness, if applicable (equal to 1 if not applicable). Prime movers with waste heat entirely in the form of exhaust (MT, MCFC and SOFC) have a pinch penalty represented by a red arrow. This accounts for the exhaust energy that cannot be utilized since it would be below the regeneration temperature of the chiller, resulting in $\varepsilon_{exh}<1$.

The way of displaying matched systems used in Figure 3 has the advantage that contours can be overlaid on it. The contours in Figure 3 represent primary energy consumption equivalent to conventional separate generation (Gluesenkamp 2012). A CCP system lying above a contour will have better primary energy ratio (PER) than the baseline conventional system. One contour has entirely optimistic assumption; the other pessimistic. The green

contour assumes that there are no heat losses from the prime mover (λ=0, where λ is defined as the fraction of fuel not converted to a useful product by the prime mover), no parasitic electricity consumption of the chiller (κ=0, where κ is defined as electrical consumption per unit of cooling), a low-efficiency baseline alternative (η=20%), and low efficiency baseline vapor compression system (COP_{VCS}=3). Compared to this baseline, all CCP systems have better PER. The other extreme baseline is shown in gray: a new combined cycle power plant driving a high efficiency vapor compression system, with high prime mover heat losses and high chiller parasitic consumption. In that scenario, only the SOFC and MCFC have better PER. All other baseline systems will lie between these two extremes, meaning that most CCP systems may or may not save energy, depending on the application.

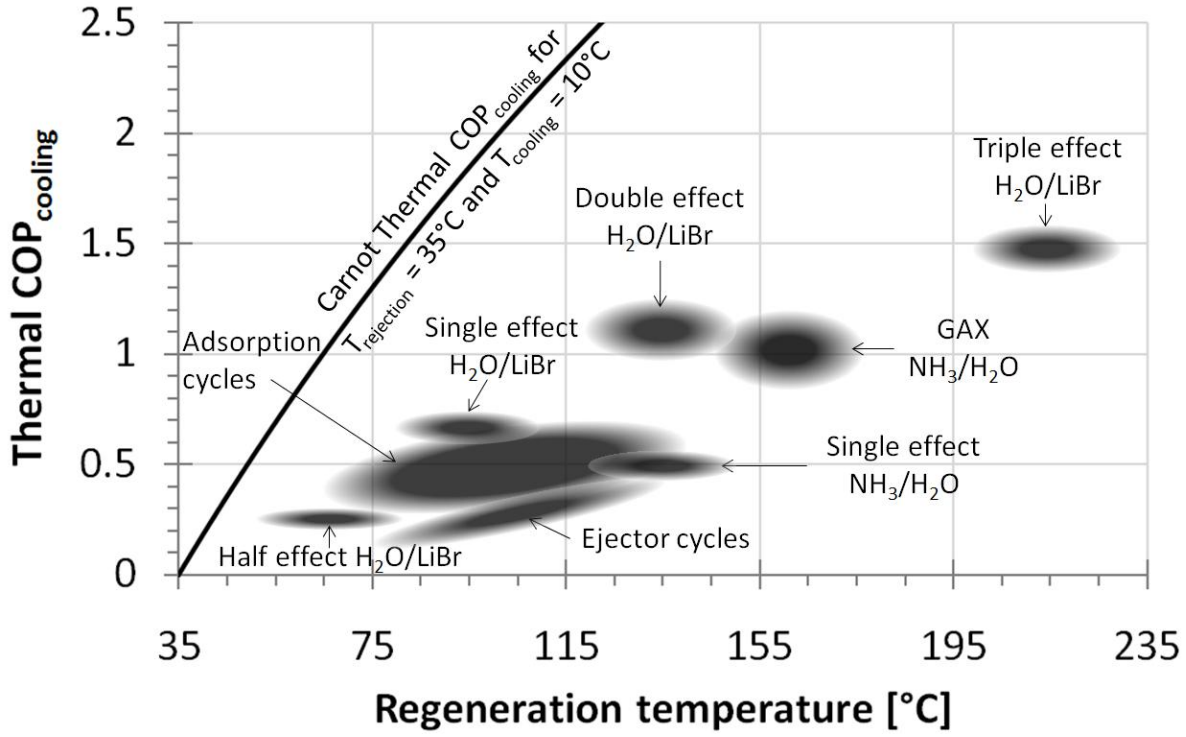

Figure 2: Thermally driven cooling technologies

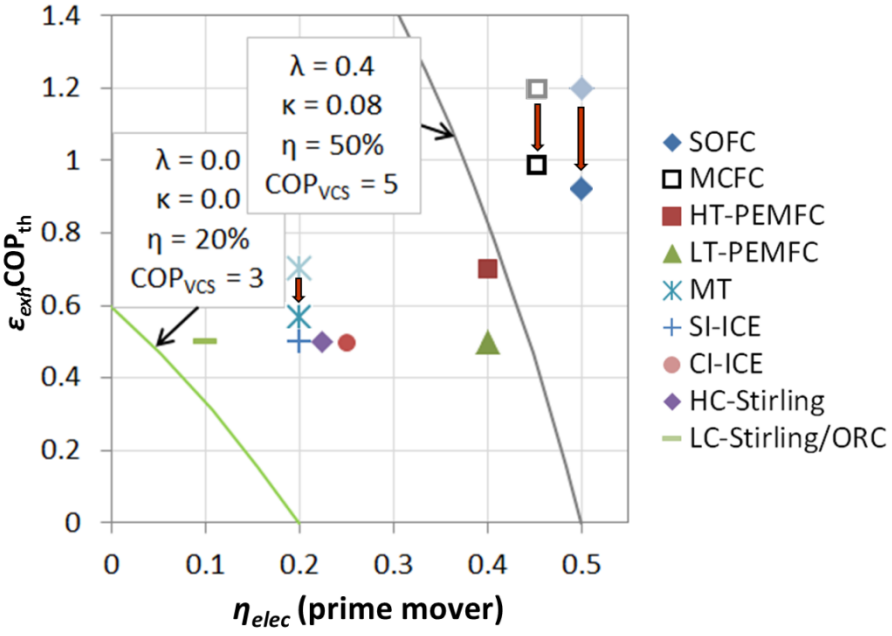

Figure 3: Matched systems and equivalent PER contours

Another way to represent matched systems is shown in Figure 4. Here the x-axis is the fuel energy consumed by the prime mover, and the y-axis is the work produced (i.e. electricity) or saved (i.e. electricity that no longer need be produced since thermally driven cooling has displaced it). Thus, the area under each curve is the net benefit of a CCP system using the given prime mover.

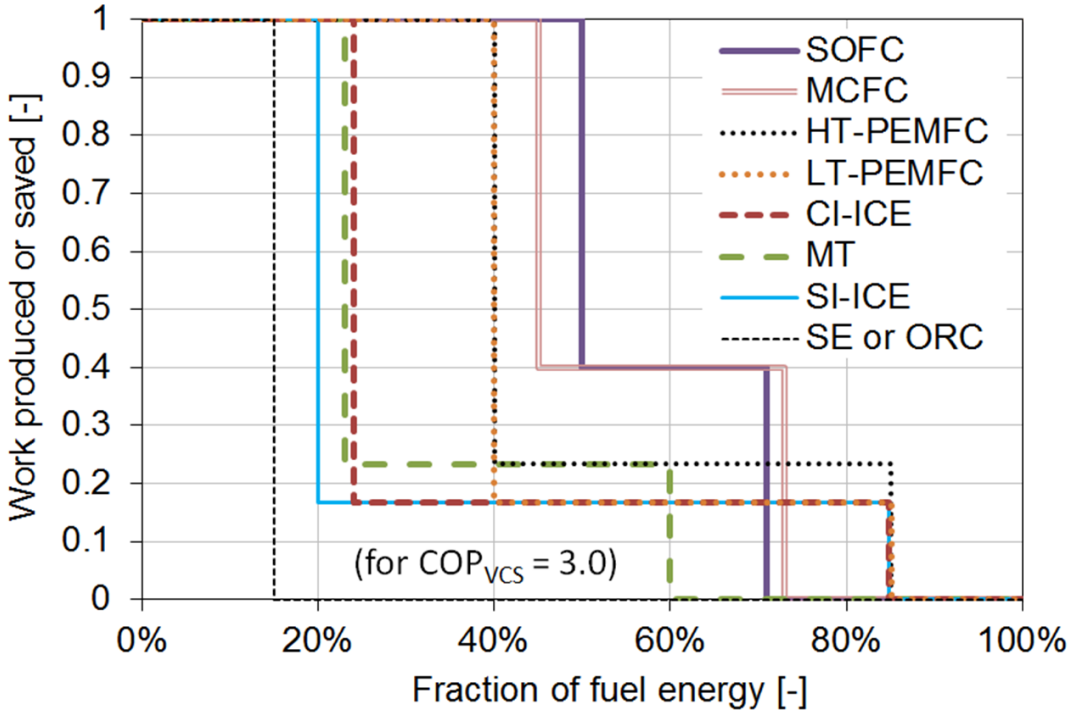

Figure 4: Work produced and saved for different CCP systems

Note that the preceding figures are optimistic since they assume that all electricity and cooling produced by a CCP system are utilized – in other words, the systems operate at the cooling fraction that naturally results from the component efficiencies. However, the relative amounts of cooling and power required by a building or process does not always match the relative amounts of cooling and power produced by a prime mover. The performance with mismatch is addressed in the next section.

3 PRIMARY ENERGY RATIO OF COMBINED COOLING AND POWER SYSTEMS WITH LOAD MISMATCH

So far, CCP systems have been assumed to operate at their natural cooling load fraction. However, the cooling demand as a fraction of the sum of cooling and electric demands (denoted f_{clg}), is highly variable with application, time of year and time of day, and thus will now be treated parametrically.

Note that, for a given match of prime mover and thermally driven chiller, there are different configurations possible. Figure 5 shows the conventional electrically-driven vapor compression cycle, and Figures 6 through 8 show three important CCP configurations.

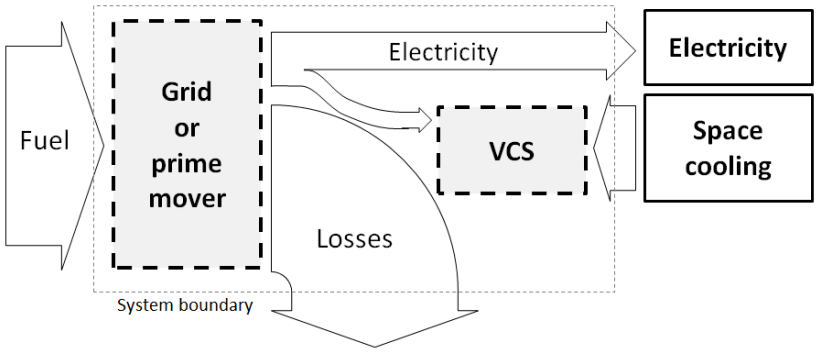

Figure 5: Conventional electrically-driven vapor compression system (VCS)

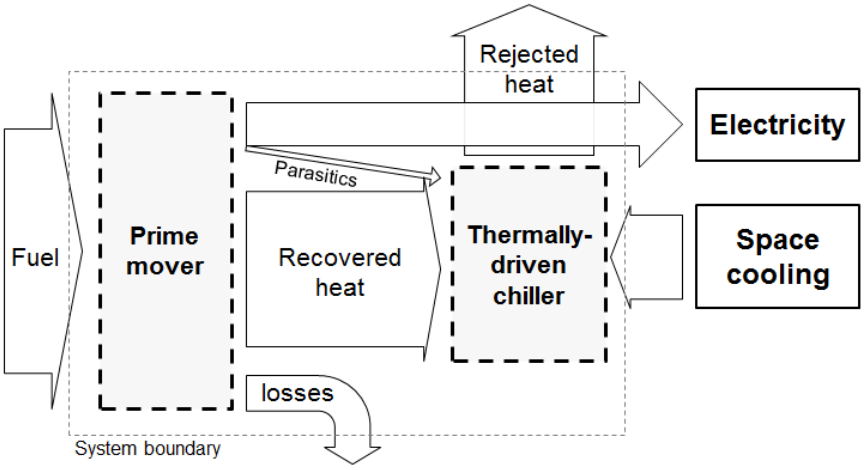

Figure 6: CCP system without backup cooling

The simple CCP schematic of Figure 6 (no backup cooling) was assumed for Figure 3. Figures 7 and 8 show two possibilities for systems with backup cooling.

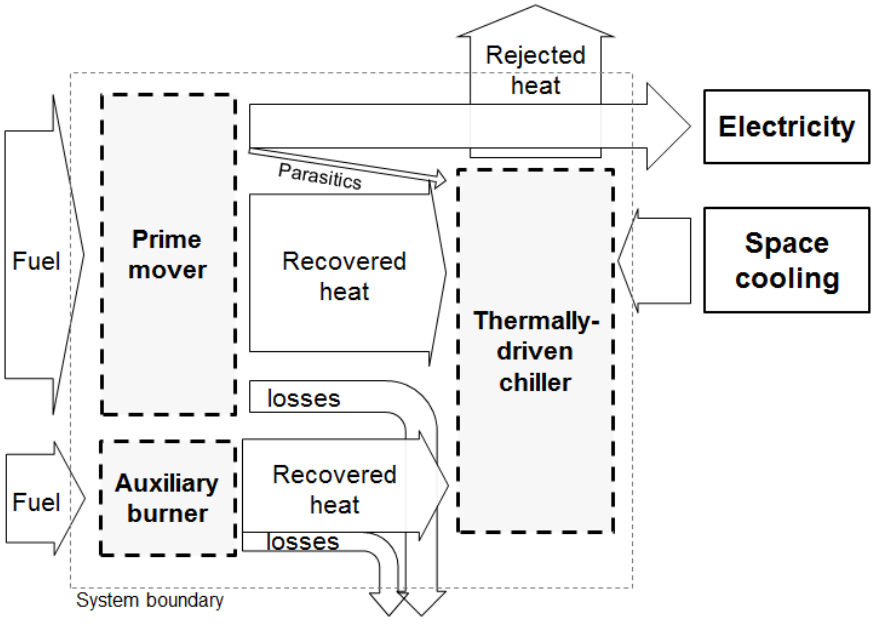

Figure 7: CCP system with auxiliary burner backup

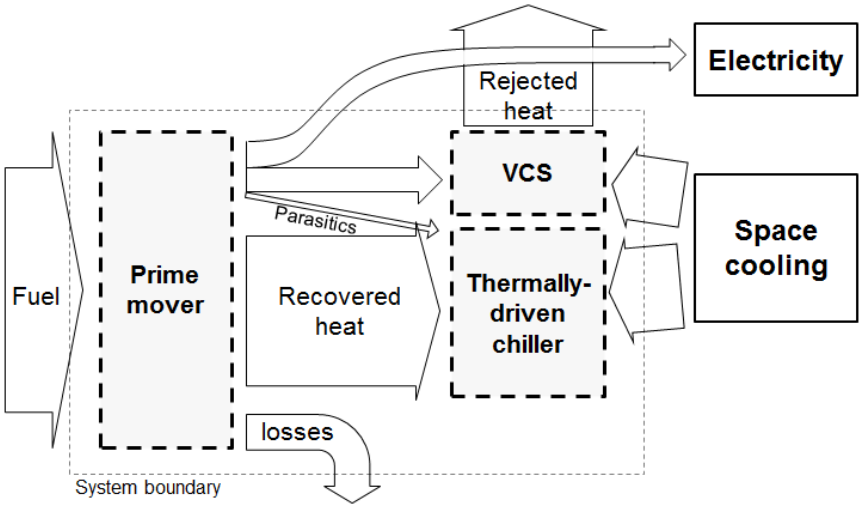

Figure 8: CCP system with backup VCS

Following the configurations shown in Figures 5 to 8, expressions can be derived for the PER of each configuration as a function of component efficiencies and the cooling demand relative to the electrical demand (Gluesenkamp 2012). In this analysis the cooling as a fraction of total load is denoted f_{clg} [-], where the total load is the sum of electrical and cooling demand [kW]. Thus f_{clg}=0 represents a demand for electricity alone, and f_{clg}=1 represents demand for cooling alone.

Using the example of a HTPEMFC prime mover, Figure 9 shows the comparison of fuel consumption (inverse PER) for conventional on-grid separate generation ("grid-VCS"), conventional off-grid separate generation (HTPEMFC-VCS), and the three CCP configurations (noAB=no auxiliary burner, wAB=with auxiliary burner). Note that inverse PER has the unit of primary energy (e.g. fuel) per unit delivered energy (cooling plus electricity): lower values represent higher efficiency systems. Using the inverse of PER allows for linear curves in the plot.

From Figure 9 it can be seen that CCP systems perform best relative to separate generation when operating at the natural cooling fraction. The value of the natural cooling fraction will vary depending on the CCP component efficiencies; for HTPEMFC it is about 0.46.

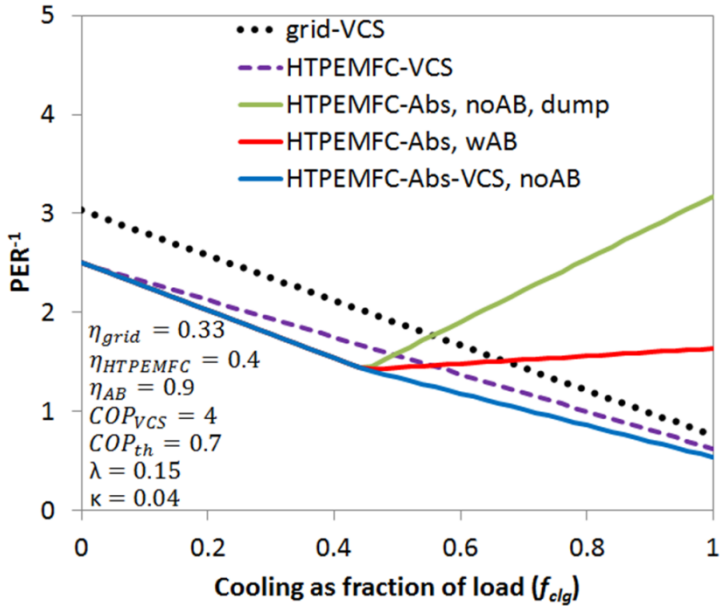

Figure 9: Inverse PER for two conventional and three CCP configurations using HTPEMFC

Figure 10 shows the same set of curves as Figure 9. For rapid visual comparison, several prime movers are shown in simplified plots. All prime movers have been assumed to have λ=0.15, and all chillers to have κ=0.04. As would be expected for typical micro (<5 kW_{elec}) devices, the prime mover electrical efficiencies are assumed to be 50% for SOFC, 40% for PEMFC, 23% for MT (assuming 25 kW_{elec} in this case), 20% for ICE, and 10% for low cost (LC) Stirling engine.

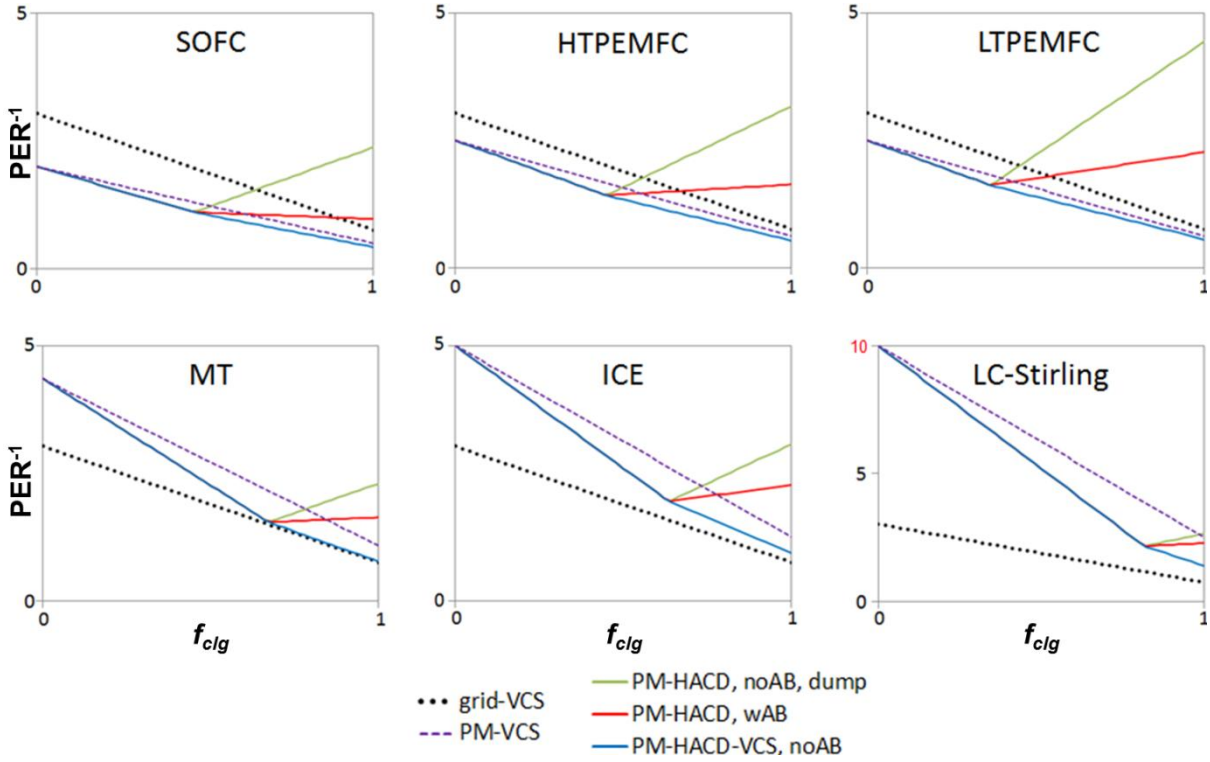

Figure 10: Inverse PER comparisons for CCP systems with various prime movers

In each plot within Figure 10, the natural cooling fraction can be seen as the point where the PER of the different CCP backup options begin to diverge with increasing cooling load fraction. Below the natural cooling fraction, systems with thermally driven cooling always have the lowest energy consumption. Above the natural cooling fraction, the VCS backup always performs best. When no backup is present, the thermally driven cooling very quickly loses its advantage above the natural cooling fraction. The burner backup is in between.

Prime movers with low electrical efficiency have the most potential for improvement by the addition of thermally driven cooling. However, the prime movers with high electrical efficiency have the best performance relative to the grid. From this it can be concluded that the greatest potential for combined cooling and power is in off-grid engines and microturbines, or on grid with fuel cells.

4 EXPERIMENTAL CCHP FACILITY AT UNIVERSITY OF MARYLAND

A prototype adsorption chiller (Qian et al. submitted) based on water and FAM-Z01 zeolite (Kakiuchi et al. 2004) was constructed and driven by waste heat from a commercially available Ecopower residential CHP engine. The engine also supplied domestic hot water to form a combined cooling, heating and power (CCHP) system. Waste heat was captured from the generator, oil cooler, cooling jackets, and exhaust, and delivered at 70°C to the chiller. The system is shown in Figure 11.

Figure 11: Photograph of combined cooling, heating and power system at UMD

The measured outputs and fuel input for the CCHP system over a 5-day load following test are shown in Figure 12 (Qian et al. 2013).

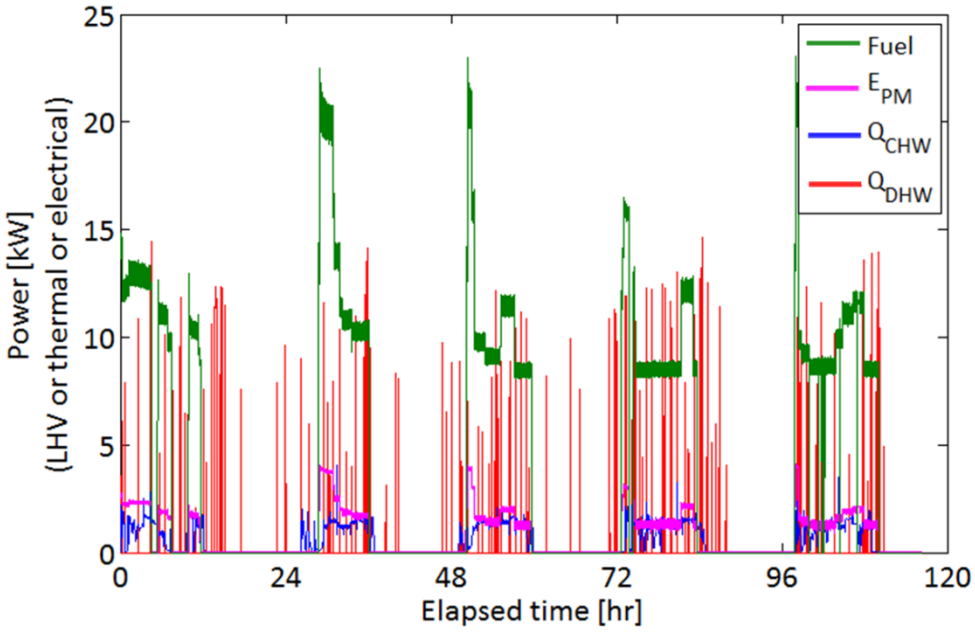

Figure 12: Measured inputs and outputs of CCHP system over 5-day load-following dynamic test

By summing the cumulative totals in Figure 12 and comparing to the primary energy that three different conventional systems would use to produce the same outputs, the savings of CCHP can be calculated, as shown in Table 1 (Qian et al. 2013). As expected from the preceding analysis, the SI-ICE based system did not save energy relative to the grid, but had substantial savings relative to a conventional off-grid system. The CCHP system also had significant savings relative to an off-grid combined heat and power system with VCS cooling.

Table 1: Fuel consumption of experimental CCHP vs. three baseline scenarios

Baseline scenario				CCHP savings
name	*electricity from:*	*DHW from:*	*cooling from:*	
grid-VCS	grid	boiler	VCS	**-15.6%**
off-grid conventional	generator	boiler	VCS	**36.1%**
off-grid CHP, VCS	CHP engine	CHP engine	VCS	**28.6%**

5 CONCLUSIONS

Thermally driven chillers can be matched with prime movers by choosing the chiller that maximizes the sum of work produced and work saved by the match. Depending on the choice of baseline system, most CCP systems may or may not save energy. Simple expressions for the PER of CCP systems can be derived as a function of the cooling load as a fraction of total load. The prime movers with the strongest potential for high efficiency are the fuel cells, especially high temperature fuel cells (SOFC, MCFC, and HTPEMFC). Conventional prime movers (ICE and MT) can save fuel in off-grid CCP systems. This was shown experimentally for an SI-ICE-based CCHP system with prototype adsorption chiller.

6 REFERENCES

Gluesenkamp, K. and Radermacher, R. 2011. “Heat Activated Cooling Technologies for Small and Micro CHP Applications,” Beith, R., ed., *Small and Micro CHP Systems*, Cambridge, UK: Woodhead Publishing Ltd.

Gluesenkamp, K. 2012. “Development and analysis of micro polygeneration systems and adsorption chillers,” PhD dissertation, University of Maryland, College Park. ProQuest/UMI. (Publication No. 3553078).

Kakiuchi, H., Iwade, M., Shimooka, S., Ooshima, K., Yamazaki, M. and Takewaki, T. 2004. “Novel zeolite adsorbents and their application for AHP and desiccant system,” *IEA Annex 17, Energy Conservation through Energy Storage, 7th Expert Meeting and Workshop*, October 8-12, Beijing, China.

Kemp, I. C. 2007. Pinch analysis and process integration: a user guide on process integration for the efficient use of energy, 2nd ed., Oxford: Butterworth-Heinemann.

Qian, S., Gluesenkamp, K., Hwang, Y., Radermacher, R. submitted to Energy. "Characterization of cyclic steady state performance and development of control strategy for adsorption chiller driven by engine coolant waste heat".

Qian, S., Gluesenkamp, K., Hwang, Y., Radermacher, R. 2013. "Experimental study on performance of a residential combined cooling, heating and power system under varying building load", *Proc. of ASME 2013 7th Int. Conf. on Energy Sustainability and 11th Fuel Cell Science, Engineering and Technology Conference*, Minneapolis, July 14-19, MN, USA.

Part of

Thermally driven heat pumps for heating and cooling. – Ed.: Annett Kühn – Berlin: Universitätsverlag der TU Berlin, 2013

ISBN 978-3-7983-2686-6 (print)
ISBN 978-3-7983-2596-8 (online)

urn:nbn:de:kobv:83-opus4-39458
[http://nbn-resolving.de/urn:nbn:de:kobv:83-opus4-39458]